

Strong correlation induced charge localization in antiferromagnets

Zheng Zhu¹, Hong-Chen Jiang², Yang Qi¹, Chu-Shun Tian¹, and Zheng-Yu Weng^{1*}

¹*Institute for Advanced Study, Tsinghua University, Beijing, 100084, China*

²*Kavli Institute for Theoretical Physics, University of California, Santa Barbara, CA, 93106-4030, U.S.A.*

* *corresponding author; email: weng@tsinghua.edu.cn*

The fate of an injected hole in a Mott antiferromagnet is an outstanding issue of strongly correlated physics. It provides important insights into doped Mott insulators closely related to high-temperature superconductivity in cuprates [1–3]. Here, we report a systematic numerical study based on the density matrix renormalization group (DMRG). It reveals a remarkable novelty and surprise for the single hole's motion in otherwise well-understood Mott insulators. Specifically, we find that the charge of the hole is self-localized by a novel quantum interference mechanism purely of strong correlation origin [4, 5], in contrast to Anderson localization due to disorders [6]. The common belief of quasiparticle picture is invalidated by the charge localization concomitant with spin-charge separation: the spin of the doped hole is found to remain a mobile object. Our findings unveil a new paradigm for doped Mott insulators that emerges already in the simplest single hole case.

A critical step in understanding the physics of doped Mott insulators is to investigate the motion of a single hole in Mott antiferromagnets [2–5, 7–19]. It is easy to imagine that an injected hole in an antiferromagnetically ordered state leaves on its path the trace of spin mismatches in the staggered magnetization direction (to be called “ S^z -string” below). Such S^z -string was expected [20] to cause the localization of the hole, but, as was later realized [9], it can be self-healed via quantum spin flips. It was then conjectured [8, 9, 11, 12] that a quasiparticle picture should be still valid in long-distance, as if the Bloch theorem holds true even for such a many-body system. The quasiparticle picture was further supported by finite-size exact diagonalizations [13] on lattices up to 32 sites [14]. However, experimentally, in angle-resolved photoemission spectroscopy (ARPES) studies [21–23], very broad single-particle spectral features have been observed in parent Mott insulator materials such as $\text{Ca}_2\text{CuO}_2\text{Cl}_2$ and $\text{Sr}_2\text{CuO}_2\text{Cl}_2$. They cast a serious doubt [15, 18] on the rationale of understanding an individual hole created by the photon within a quasiparticle description. Furthermore, the charge localization is a general phenomenon for a lightly doped cuprate before the system becomes a high- T_c superconductor. Whether the localization here is intrinsic or due to the presence of disorders remains unsettled.

Theoretically, the validity of a quasiparticle description has been questioned in the literature as well. It was first argued by Anderson [10] on general grounds that the quasiparticle spectral weight should vanish due to an unrenormalizable many-body phase shift induced when a hole is injected into a Mott insulator. Later, the discovery of the so-called phase string [4, 5] leads to a microscopic justification of this crucial observation. Here, a phase string may be regarded as an S^\pm -string as opposed to the aforementioned “ S^z -string”. It is irreparable by quantum spin flips in contrast to the S^z -string. It was further predicted [18] that the phase string, instead of the S^z -string [20], is responsible for an intrinsic self-localization of the injected hole in two dimensions.

In this work, a large-size numerical simulation is used as a powerful machinery to resolve this issue. This approach is of particular importance because the hole's motion is highly sensitive to quantum interference developing at long distance. To this end, we study the ladder systems by the DMRG method

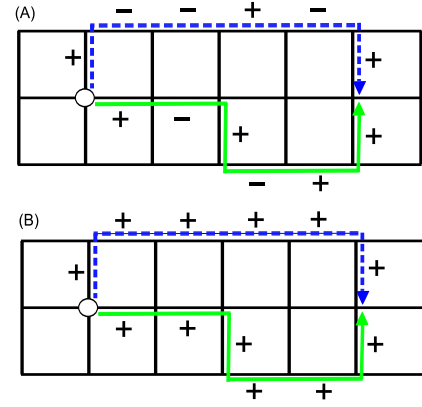


Fig. 1: Quantum interference picture of one hole in the t - J model (A): As the hole moves from the injection point to a distant site, a sign sequence – the phase string [4, 5] – is left behind as exemplified by the solid (green) and dashed (blue) lines. Here each $+$ ($-$) sign faithfully records an event that the hole exchanges its position with the nearest neighboring \uparrow (\downarrow) spin during its motion. (B) By contrast, the phase string can be wholly switched off in the $\sigma \cdot t$ - J model (see the text) such that the amplitude associated with each path is positive definite (of the same absolute magnitude as in the t - J model). The presence (absence) of phase strings will drastically alter the long-wavelength behavior of the hole via quantum destructive (constructive) interference as demonstrated in this work.

[24], in which the length scale along one direction can be sufficiently large. As a ladder sample is long enough, we find that the charge is generally localized so long as the leg number is larger than one. The localization scale decreases monotonically as the leg number increases, suggesting a stronger self-localization in the two dimensional limit. Contrary to this, if the sample is not long enough, the injected hole behaves itinerantly, implying that the quasiparticle picture found in earlier numerical studies [13, 14] is likely a small-size effect. We further show that complementary to the charge localization, the system exhibits novel spin-charge separation. That is, the “spinon” that carries the spin quantum of the doped hole remains mobile. We demonstrate that both charge self-

localization and spin-charge separation find their origin in the phase string, a unique property of the t - J model [4, 5, 25]. As a further evidence, we find that all of these exotic properties disappear once the phase string is turned off artificially in the simulation, and a well-defined quasiparticle description is recovered in consistency with the common wisdom [9] of spin polaron picture.

Models and methods.— A prototypical doped Mott insulator is described by the t - J Hamiltonian, $H_{t-J} = H_t + H_J$, with

$$\begin{aligned} H_t &= -t \sum_{\langle ij \rangle \sigma} (c_{i\sigma}^\dagger c_{j\sigma} + h.c.), \\ H_J &= J \sum_{\langle ij \rangle} (\mathbf{S}_i \cdot \mathbf{S}_j - \frac{1}{4} n_i n_j). \end{aligned} \quad (1)$$

Here, $c_{i\sigma}^\dagger$ is the electron creation operator at site i , \mathbf{S}_i the spin operator, and n_i the number operator. The summation is over all the nearest-neighbors, $\langle ij \rangle$. The Hilbert space is constrained by the no-double-occupancy condition, i.e., $n_i \leq 1$. At half-filling, $n_i = 1$, the system reduces to Mott insulators (antiferromagnets) with a superexchange coupling, J . Upon doping a hole into this system, $\sum_i n_i = N - 1$ (N the number of the lattice sites), and the hopping process is triggered as described by the hopping term, H_t , with t the hopping integral.

For the single hole doped t - J model in a bipartite lattice, there exists an exact theorem, which states [4, 5, 25] that the propagation of the hole is a superposition of quantum amplitudes of all the paths, with each path carrying a unique sign sequence known as the phase string, i.e.,

$$(+1) \times (-1) \times (-1) \times \dots \quad (2)$$

Here, the sign \pm on the right-hand side keeps track of an \uparrow or \downarrow -spin exchanged with the hole at each step of hopping as illustrated in Fig. 1 (A).

The quantum interference of phase strings from different paths is expected to be strong and play the fundamental role in dictating the long-distance behavior of the hole. In order to uniquely pin down the effect of phase strings, we also introduce the so-called $\sigma \cdot t$ - J model with the hopping term H_t in Eq. (1) replaced by

$$H_{\sigma \cdot t} = -t \sum_{\langle ij \rangle \sigma} \sigma (c_{i\sigma}^\dagger c_{j\sigma} + h.c.), \quad (3)$$

(i.e., an extra sign $\sigma = \pm 1$ is added). It is easy to show, following Refs. [4, 5, 25], that the phase string (2) disappears, whereas the positive weight for each path remains unchanged [as illustrated in Fig. 1 (B)]. In other words, one can artificially switch on and off the phase string effect between the t - J and $\sigma \cdot t$ - J models to study its novel consequences.

Previously the DMRG algorithm has already been used to study the t - J model in ladder systems at low hole doping [17, 26]. Below we shall focus on the one hole case on bipartite lattices of $N = N_x \times N_y$, where N_x and N_y are the site numbers in the x and y directions, respectively. By using the DMRG method, we shall study the ladders with small N_y

(from 1 to 5) and sufficiently large N_x . Here we set J as the unit of energy and focus on the $t/J = 3$ case unless otherwise specifically stated. Enough numbers of states in each DMRG block are kept to achieve a good convergence with total truncation error of the order of $10^{-8} - 10^{-12}$.

Self-localization of the charge.— Typical examples of the hole density distribution, $\langle n_i^h \rangle \equiv 1 - \langle n_i \rangle$, are shown in Fig. 2 (A) and (B) for $N_y = 3$ and 4, respectively. Here the charge profiles are plotted along the x direction for a middle leg of the ladders. They are localized in the central region of the ladders with open boundaries. Upon summing up the distribution at all the sites of different legs, the sum rule: $\sum_i \langle n_i^h \rangle = 1$ is satisfied. Examples of the contour plot of $\langle n_i^h \rangle$ in the x - y plane can be found in Fig. S3 in Supplementary Information.

One may systematically change the ladder length N_x to study the full width at half-maximum (FWHM) of the charge profile. Fig. 2 (C) shows that for ladders with different N_y , the FWHM increases linearly for small sample lengths, while saturates for sufficiently large sample lengths (except the $N_y = 1$ case). The former indicates that the doped hole still remains itinerant at a smaller N_x . The latter suggests that a self-localization takes place for the doped hole, when the ladder length is long enough where the FWHM is no longer sensitive to the boundaries along the x -direction. Later on, by a more precise analysis, it will be shown that such localization only involves the charge of the doped hole, not its spin. Furthermore, Fig. 2 (C) clearly shows that the saturated FWHM at $N_y > 1$ monotonically decreases with the increase of the leg number N_y , implying even stronger localization in the two-dimensional limit. By contrast, there is no indication of saturation in FWHM for long one-dimensional chains ($N_y = 1$, with N_x up to 500), which is consistent with the fact that the doped hole in strictly one dimension exhibits the Luttinger liquid behavior [2].

The destructive quantum interference effect of phase strings in the t - J model provides a natural explanation for the charge “self-localization” observed in the above DMRG results. To further confirm the phase string origin of self-localization, we switch off the phase string interference by two methods and then repeat the previous procedure of numerical simulations. In the first method, we study the $\sigma \cdot t$ - J model introduced above. In the second method, we set the interchain hopping coefficient, t_\perp , to be zero such that the hole can only move in the x -direction as if in a one-dimensional chain. In both cases, the interference picture shown in Fig. 1 (A) breaks down. The numerical results for these two models are presented in Fig. 2 (D) for two- and three-leg cases, in which the FWHM of the hole density distribution restores the behavior of linear increase with the sample length. It indicates that the charge becomes delocalized in both cases, in sharp contrast to the self-localization in the t - J model.

Although the observed self-localization is insensitive to the parity (even-odd) of the leg number, the hole distribution is, as shown in Fig. 2 (A) and (B) and Supplementary Information: for the even-leg ladders ($N_y = 2, 4$), there are always small spatial oscillations on top of the Gaussian density profile, while they are absent for the odd-leg ladders ($N_y = 3, 5$). This can be attributed to distinct decaying behavior of spin-

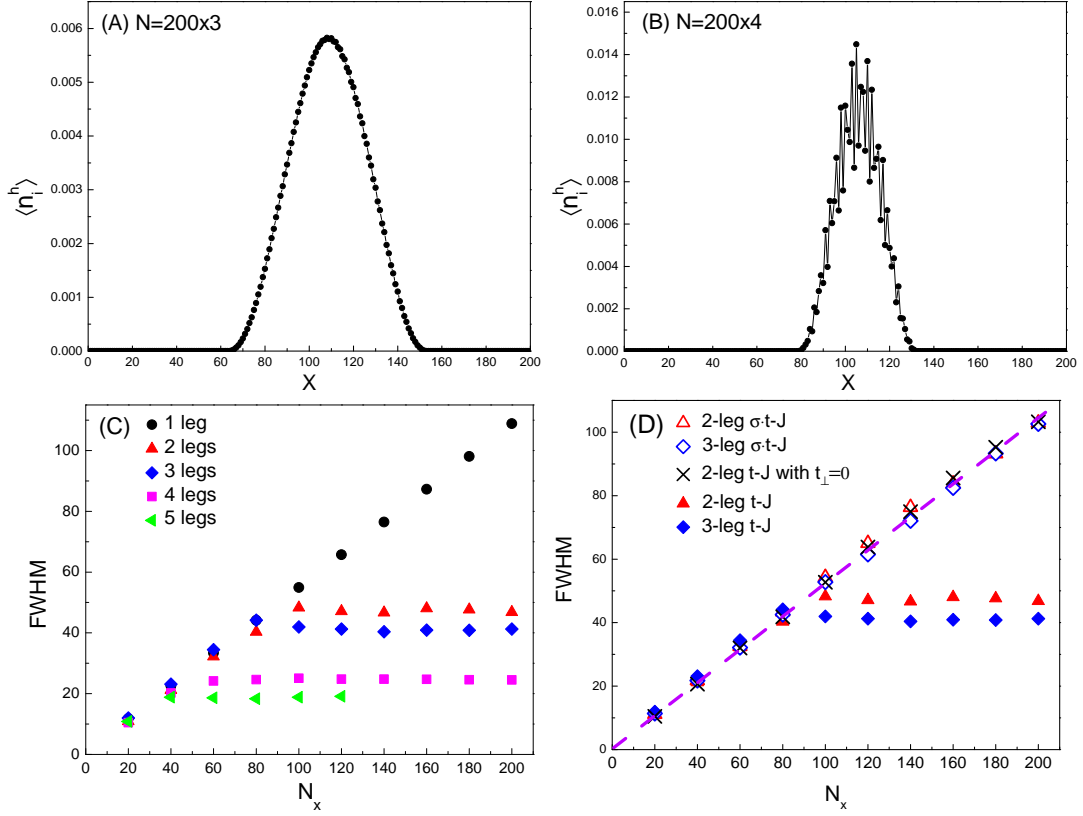


Fig. 2: Self-localization of the charge in a 3-leg ladder system of size $N = 200 \times 3$ (A) and 4-leg ladder of $N = 200 \times 4$ (B). The density distribution $\langle n_i^h \rangle$ along the x axis in a middle leg is well fitted by the Gaussian function with a full width at half-maximum (FWHM). (C) The behavior of FWHM depends on the leg number N_y : for the ladders of $N_y > 1$, the FWHM first increases linearly at small N_x and then saturates at large N_x , with a length scale monotonically decreasing with the leg number; for $N_y = 1$, the FWHM grows unboundedly as the sample length increases. (D) Delocalization of the charge in the absence of phase string interference for the two modified models, namely the $\sigma \cdot t$ -J model and the t -J model with interchain hopping coefficient $t_\perp = 0$. The corresponding FWHM unboundedly increases with N_x (open triangles, open diamonds, and crosses). The dashed line ($= N_x/2$) is a guide to the eye.

spin correlations for the odd- and even-leg ladders at half-filling: the former (latter) follows a power (an exponential) law reflecting the absence (presence) of spin gap, see Supplementary Information for further explanations. Furthermore, the distinction of the even-odd effect disappears with the increase of t/J ratio (see Fig. S4), indicating that the detailed spin dynamics, governed by J , is not essential to the charge self-localization effect.

Momentum distribution.— Now let us examine the momentum distribution of the hole by studying $n(\mathbf{k}) \equiv \sum_\sigma \langle c_{\mathbf{k}\sigma}^\dagger c_{\mathbf{k}\sigma} \rangle$, which can be obtained by a Fourier transformation of $\sum_\sigma \langle c_{i\sigma}^\dagger c_{j\sigma} \rangle$. At half-filling, one finds $n(\mathbf{k}) = 1$ and for the one hole case, $1 - n(\mathbf{k})$ is shown in Fig. 3.

The insets of Fig. 3 (A) and (B) present the hole momentum distribution $1 - n(\mathbf{k})$ as a function of k_x for fixed $k_y = 2\pi/3$ in the 3-leg ladder and $k_y = \pi/2$ in the 4-leg ladder, respectively. The value of k_y is chosen in a way that the “sudden change” in $1 - n(\mathbf{k})$ can reach maxima by varying k_x , according to the contour plots in the k_x - k_y plane (see Supplementary Information). A very interesting feature is that after the rescaling: $1 - n(\mathbf{k}) \rightarrow [1 - n(\mathbf{k})]N$, all the curves in the inset of

Fig. 3(A) [or (B)] collapse onto a universal curve shown in the corresponding main panel. If one defines the Fermi surface by the sudden jump in the momentum distribution function, then the two universal curves suggest that the quasiparticle spectral weight is upper-bounded by $1/N$ for large N , and vanishes in the thermodynamic limit.

To satisfy the sum rule, $\sum_{\mathbf{k}} (1 - n(\mathbf{k})) = 1$, the width of the jump in $1 - n(\mathbf{k})$ must remain finite in the limit $N \rightarrow \infty$. This is clearly shown in Fig. 3 (A) and (B), consistent with a finite localization length in the real space. We have also calculated the hole momentum distribution at different ratios of t/J . As shown in Supplementary Information, for a given sample size, the jump near the Fermi point is continuously reduced with increasing t/J , which is qualitatively consistent with earlier work [13].

Again a sharp contrast arises once the phase string is turned off in the $\sigma \cdot t$ -J model, as shown in Fig. 3(C) for the 4-leg ladder. Here the wide spread of $1 - n(\mathbf{k})$ in the momentum space seen in (A) and (B) collapses into a sharp peak at $k_x, k_y = 0$. In particular, a universal curve (the inset) is obtained by the rescaling: $k_x \rightarrow N_x k_x$ instead of by $1 - n(k) \rightarrow [1 - n(\mathbf{k})]N$

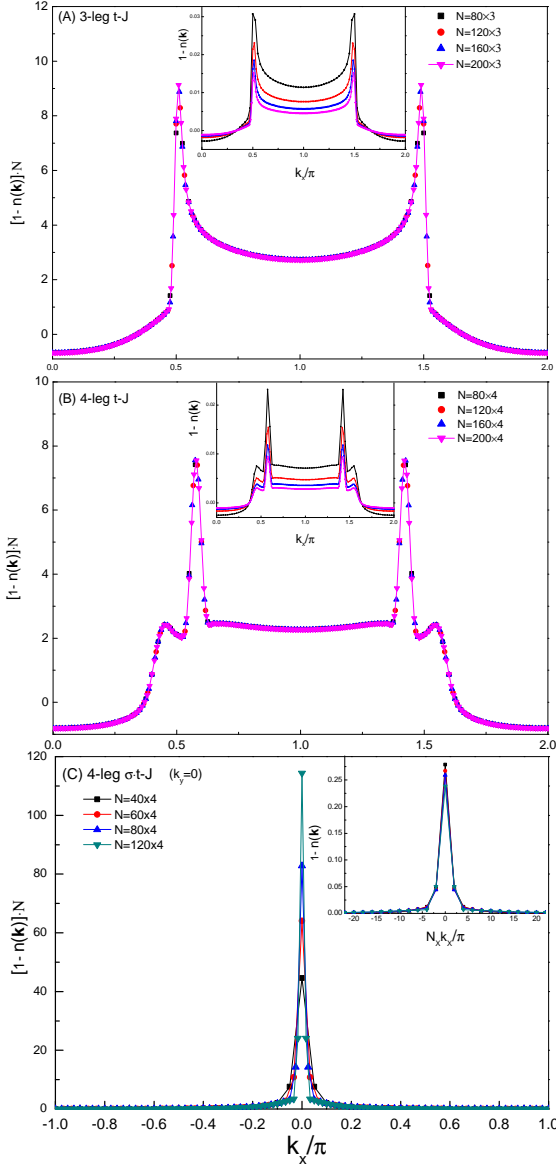


Fig. 3: Momentum distribution. For both 3-leg (A) and 4-leg (B) ladders, the momentum distribution of the hole exhibits scaling behavior: after the rescaling, $1 - n(\mathbf{k}) \rightarrow [1 - n(\mathbf{k})]N$, the curves at different sample lengths in the inset collapse onto a single one represented in the corresponding main panel. Note that we fix $k_y = \frac{2\pi}{3}$ for the 3-leg case and $k_y = \frac{\pi}{2}$ for the 4-leg case, and plot the distribution along k_x . Representative contour plots in the whole k_x - k_y plane are shown in Fig. S5 (Supplementary Information). (C) The quasiparticle picture is recovered for the $\sigma \cdot t$ - J model. The main panel shows that the momentum distributions of different sample lengths collapse to a single momentum at $k_x = k_y = 0$ for the 4-leg ladder; The inset shows that a universal curve is obtained for $1 - n(\mathbf{k})$ after the rescaling: $k_x \rightarrow N_x k_x$, which suggests a nonvanishing quasiparticle spectral weight peaked at $\mathbf{k} = 0$.

as done in the main panel. This clearly indicates that the quasiparticle spectral weight is finite and a Bloch-like state is restored with a definite momentum at $\mathbf{k} = 0$ (a peak at the equivalent of $k_x, k_y = \pi$ is also found).

Spin-charge separation.— Complementary to the charge localization illustrated in Fig. 2, we further explore the fate of the spin-1/2 associated with the hole injected into the half-filled spin-singlet background.

For the 3-leg ladder, the existence of spin-charge separation is explicitly demonstrated by Fig. 4(A). Here the single hole is created by removing a \downarrow spin electron. While the charge of the doped hole is well localized at the sample center, the extra spin of $S^z = 1/2$ spreads over the sample. It is indicated by spin density $\langle S_i^z \rangle$ as well as the coarse grained $\langle S_i^z \rangle_{c.g.}$, which is approximately uniform across the ladder. This is probably the most direct display of electron fractionalization for a doped Mott insulator, thanks to the charge localization. Note that it is very different from the well-known one-dimensional Luttinger liquid, where both charge (holon) and spin (spinon) are mobile [2].

For an even-leg ladder, the presence of a spin gap in the spin background renders the spin-charge separation less explicit because the extra spin of $S^z = 1/2$ will also tend to stay in the hole region in order to reduce its superexchange energy cost, as illustrated in Fig. 4(B) for the 2-leg ladder case. To directly observe a similar spin-charge separation picture in an even-leg ladder, the spin gap has to be small enough, a condition that can be achieved only if the leg number is sufficiently large. In this limit, the behavior of the single hole in both even- and odd-leg ladders is expected to converge with a stronger charge localization.

Nevertheless, the spin-charge separation in the 2-leg ladder can be well confirmed by a different method. Note that, first, if the charge part – namely the holon – is localized, the localization center can be anywhere in a translationally invariant system. In particular, an “extended” profile as a linear superposition of the localized wave packets at different positions should be also energetically degenerate. Second, if Fig. 4(B) really corresponds to spin-charge separation, the extra spin-1/2 – namely the spinon – should be more or less “free” within the regime expanded by the charge distribution. Then the spinon will prefer a more extended distribution of the hole to further lower its energy. In other words, the degeneracy of localized states should be lifted in favor of an extended profile in order to gain additional spinon energy.

Indeed, by increasing DMRG sweep number with the truncation error reaching much lower than 10^{-8} , the localized profile in Fig. 4(B) is found to slowly converge to an extended one as shown in (C) with the total energy lowered by $\sim 10^{-4}J$. To identify the nature of this small energy gain, one may vary the sample size from $N_x = 16$ to 800, and repeat the same procedure to obtain the one-hole energy $E_G^{1\text{-hole}}$ at each N_x [with the same full convergence to the extended charge profile as in Fig. 4(C)]. As shown in the inset of Fig. 5(A), with a constant term excluded, $E_G^{1\text{-hole}}$ is well fitted by $\alpha(\pi/N_x)^2$ (blue triangles) with the coefficient $\alpha = 0.87J$, as if it is contributed by some “free particle” in a box of length N_x [27].

Next, we show that such $1/N_x^2$ (finite-size) contribution to

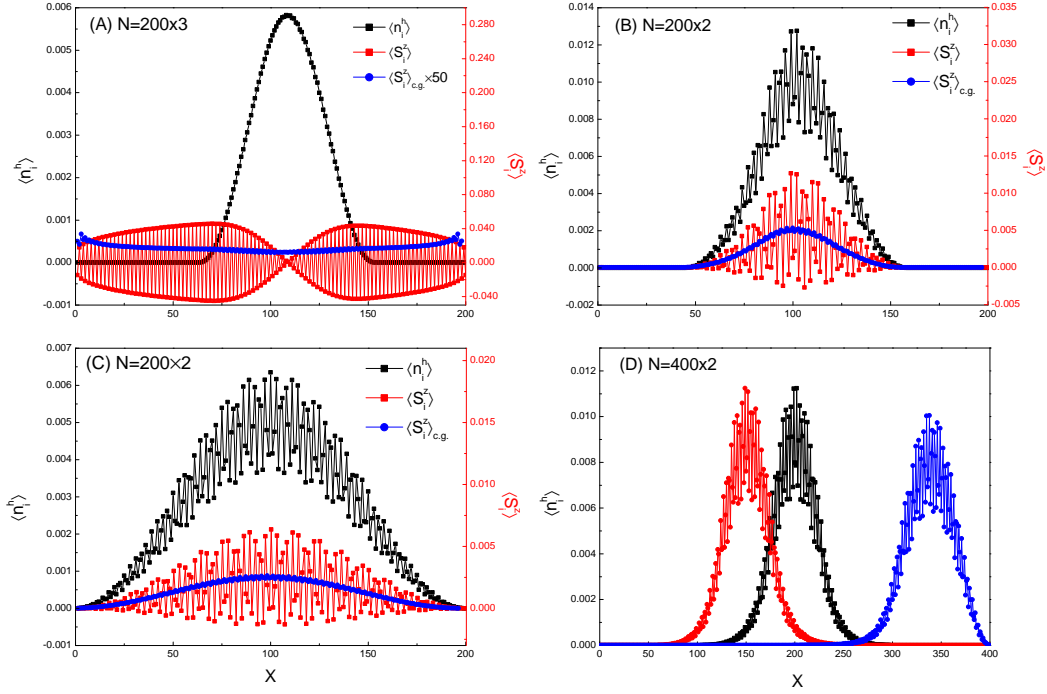


Fig. 4: (A) Spin-charge separation in a 3-leg ladder with a \downarrow spin electron removed. The charge of the hole is localized at the sample center and the spin of $S^z = 1/2$ spreads over the entire sample, with the coarse grained density $\langle S_i^z \rangle_{c.g.}$ approximately uniform. (B) In a 2-leg ladder, the charge and spin of the doped hole remain in the same localized region because of a finite spin-gap in the spin background. (C) An extended profile of the charge can be obtained with further reducing DMRG truncation error (see the text); In this case, although the charge remains localized, the mobile spinon gains a tiny additional energy (cf. Fig. 5). (D) In a $N = 400 \times 2$ ladder, by adding weak chemical potentials the hole density can be localized anywhere along the ladder.

$E_G^{1\text{-hole}}$ is not from the charge sector. For this purpose, we make the 2-leg ladder as a ribbon by connecting the boundaries on the two edges of the ladder in the x -direction. Then we calculate the energy difference $\Delta E_G^{1\text{-hole}} \equiv E_G^{1\text{-hole}}(\pi) - E_G^{1\text{-hole}}(0)$ with threading through a flux π into the ribbon. It corresponds to the change of boundary condition from the periodic to anti-periodic one for the hopping term and is equivalent to coupling a small electric field to the charge sector. As shown in Fig. 5(A), $\Delta E_G^{1\text{-hole}}$ oscillates strongly and falls off exponentially as $e^{-N_x/\xi}$ with $\xi \sim 14.5$. It behaves completely different from $1/N_x^2$ behavior exhibited in $E_G^{1\text{-hole}}$, indicating that the charge indeed remains localized. The “free particle-like” behavior in $E_G^{1\text{-hole}}$ should therefore solely originate from the charge-neutral part of the doped hole, i.e., the spinon.

By a sharp contrast, upon turning off the phase-string in the $\sigma \cdot t$ - J model, both $E_G^{1\text{-hole}}$ and $\Delta E_G^{1\text{-hole}}$ follow the same $1/N_x^2$ behavior as clearly shown in the inset of Fig. 5(A). It is consistent with the previous conclusion that in this case the doped hole is restored as a quasiparticle, which carries both charge and spin and thus responds very similarly to the boundary condition (i.e., the finite-size effect) as a single mobile object.

The spin-charge separation is well-known for the one-dimensional chain [2]. Figure 5(B) presents the corresponding 1-leg results. As shown in the inset, the finite-size effect of $E_G^{1\text{-hole}}$ ($\propto 1/N_x^{1.5}$) is indistinguishable from the phase string

free case (with open boundary conditions). But the charge response of $\Delta E_G^{1\text{-hole}}$ is again totally different [the main panel of Fig. 5(B)]. It oscillates strongly as a function of N_x , similar to the 2-leg case in Fig. 5(A). As a matter of fact, it can be directly attributed to the phase string modulation in the expression for the ground state energy given in Ref. [18]. The main difference from the 2-leg case is that the envelop of $\Delta E_G^{1\text{-hole}}$ decays with increasing N_x in a power law fashion ($\propto 1/N_x^3$) instead of an exponential one. This is consistent with the fact that the holon is not localized in the one-dimensional case. It is interesting to notice that even without the phase string effect, $E_G^{1\text{-hole}}$ and $\Delta E_G^{1\text{-hole}}$ behave distinctly for the $\sigma \cdot t$ - J model. The former $\propto 1/N_x^{1.5}$, while the latter $\propto 1/N_x^2$, also indicating a spin-charge separation although the distinction is much less dramatic as compared to the t - J model.

The presence of spin-charge separation enriches substantially the behavior of the hole localized states in the t - J ladder systems. Due to the residual spin-charge interaction, the degenerate charge localized states are superposed to form a more “extended” distribution to minimize the spinon energy. It has been shown [28] that generally the DMRG method tends to pick up a *minimally entangled* state among quasi-degenerate states. Thus, spatially localized ones such as those in Fig. 2 are naturally obtained because a further spinon energy gain for a bigger FWHM would be too tiny to be detected with

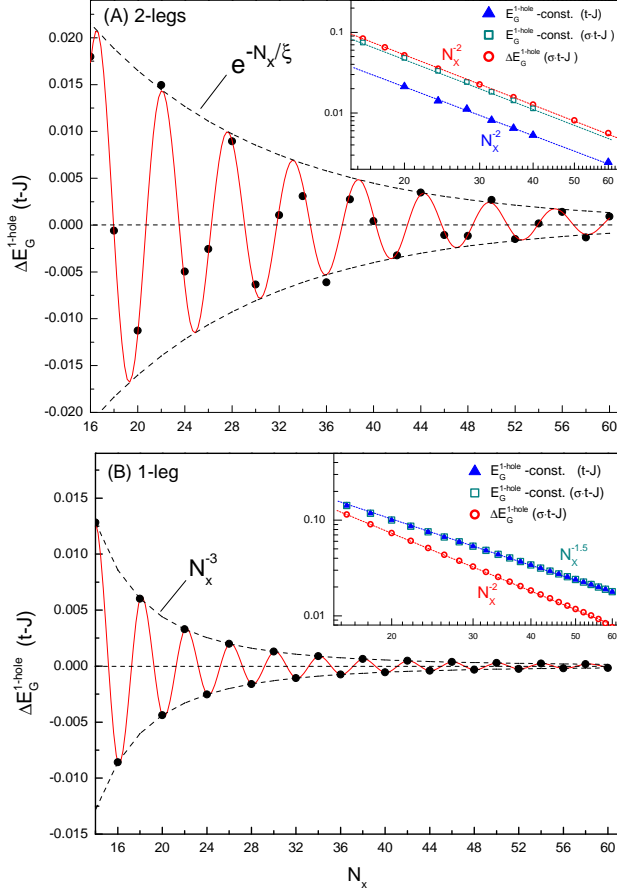


Fig. 5: The energy difference ΔE_G^{1-hole} between anti-periodic and periodic boundary conditions along the x -direction for the charge shows an oscillation vs. N_x , which is a direct manifestation of the phase string effect. The exponential decay of the envelop (dashed curves) of ΔE_G^{1-hole} shows the charge localization for the 2-leg ladder (A), while the power law decay for the 1-leg ladder case (B) indicates a Luttinger liquid behavior. By sharp contrast, in the inset of (A), a completely different finite-size behavior ($1/N_x^2$) is exhibited in the ground state energy E_G^{1-hole} for the 2-leg ladder, confirming the spin-charge separation. For comparison, both ΔE_G^{1-hole} and E_G^{1-hole} follow the same $1/N_x^2$ dependence once the phase string is turned off, as shown in the inset of (A), where the quasiparticle picture is restored with a spin-charge recombination. In the inset of (B), similar comparisons for the 1-leg case are presented.

a given small DMRG truncation error. It also explains why the FWHM of charge distribution shown in Figs. 2 and 4 is usually bigger than the intrinsic localization length ξ as exhibited by ΔE_G^{1-hole} . But the former is still valid to characterize the general trend of the localization, say, as a function of the leg number in Fig. 2. On the other hand, by adding some weak local chemical potentials, the quasi-degeneracy of the hole states can be lifted such that the hole density profile

is truly localized around the impurities at different locations [as indicated by different colored curves in Fig. 4(D) for a $N = 400 \times 2$ ladder]. Here the increase of the total energy of the original t - J Hamiltonian is weak (about $10^{-4}J$), presumably from the spinon part as the FWHM is still larger than ξ .

Discussions.— Phase string, charge localization, and spin-charge separation are striking results of a single-hole-doped Mott insulator. They are truly incompatible with a quasiparticle description. However, for their novel effects to get fully unveiled, a large sample is needed. Instead of tackling directly a two-dimensional square lattice, in this work, we have chosen ladders that DMRG can access. As it turns out, very surprising consequences do show up so long as the ladders are long enough, *and*, there are more than one paths to realize quantum interference, e.g., in a two-leg system.

The most essential physics underlying the observed exotic phenomena is that the motion of the single hole acquires a sequence of signs that precisely and permanently record each microscopic *hole-hopping-spin-backflow* event in the quantum spin background. These irreparable phase strings cause singular and destructive interference of quantum waves of the charge. The longer the paths are, the stronger the destructive interference is. The present results show unequivocally that the self-localization of the charge is a combined effect of quantum interference and multiple scattering between the doped charge and spin background, in analogy to Anderson localization [6]. Contrary to this, the charge remains delocalized in the single chain case due to the lack of quantum interference involving *different* paths.

The charge localization is further found to be concomitant with spin-charge separation for the two and more-leg ladders. Whereas the phase string renders kinetic energy suppression of the charge, the spin associated with the doped hole remains unfrustrated and thus maintains a coherent motion as a spinon. This has been clearly demonstrated by the distinct finite-size effects of the charge and spin degrees of freedom. In this sense, the electron fractionalization found in the single hole case can be attributed to the energetic reason. Note that the cause for charge localization, i.e., the nontrivial phase string effect, requires an uncertainty of the spin quantum associated with the spin backflow (leading to the \pm signs). If *each* spin backflow could maintain a definite spin polarization direction, the phase string effect would become trivial. Simultaneously the hole would also carry a definite spin as a quasiparticle. But such a spin-charge recombination, being extremely tight in space, would cost too much kinetic energy.

This is fundamentally different from the premise for a spin polaron picture – a conventional wisdom in which the disturbance of the hole hopping to the spin background is described by virtual spin excitations that eventually relax back after the hole moves away. In fact, the spin-polaron or quasiparticle behavior has been shown to be recovered once the phase string is “switched off” in the so-called $\sigma \cdot t$ - J model, where everything seems “normal” in a conventional sense. Here a spin-charge recombination (not too tight spatially) with a good kinetic energy for the quasiparticle can be realized since there is no more singular phase string effect to strongly suppress the

kinetic energy of the charge.

Our results have far-reaching consequences. First of all, they suggest that a new state of quantum matter may naturally emerge in sufficiently low doping. Such a state is insulating because of the self-localization of doped charges, not because of a charge gap like in the undoped case. This is a novel non-Anderson-type localization phenomenon since external disorders are absent. Secondly, the strong suppression of the kinetic energy results in a large quasi-degeneracy in the low-energy states. It is expected to lead to a “glassy” behavior in the presence of weak external impurities and a “competing-order” phenomenon in the presence of additional weak interactions. It also provides a possible explanation for

the strongly localized state induced by a surface defect observed in the scanning tunneling microscope experiment on $\text{Ca}_2\text{CuO}_2\text{Cl}_2$ [29]. Thirdly, the spin background remains essentially the same as at half-filling, but the spinons fractionalized from the doped holes will play an important role to determine the low-energy, long-wavelength sector of spin dynamics in the lightly doping. Finally, given that phase strings have been proved [25] rigorously as the sole sign structure in the t - J model on bipartite lattices, regardless of doping concentration, temperature, and dimensions, the present work also provides significant insights into the long-standing issue of high temperature superconductivity at finite doping.

-
- [1] P. W. Anderson, The resonating valence bond state in La_2CuO_4 and superconductivity. *Science* **235**, 1196 (1987).
 - [2] P. W. Anderson, *The Theory of Superconductivity in the High- T_c Cuprates* (Princeton University Press, Princeton, NJ, 1997).
 - [3] P. A. Lee, N. Nagaosa and X. G. Wen, Doping a Mott insulator: Physics of high-temperature superconductivity. *Rev. Mod. Phys.* **78**, 17 (2006).
 - [4] D. N. Sheng, Y. C. Chen, and Z. Y. Weng, Phase string effect in a doped antiferromagnet. *Phys. Rev. Lett.* **77**, 5102 (1996).
 - [5] Z. Y. Weng, D. N. Sheng, Y.C. Chen, and C.S. Ting, Phase string effect in the t - J model: General theory. *Phys. Rev. B* **55**, 3894 (1997).
 - [6] P. W. Anderson, Absence of diffusion in certain random lattices. *Phys. Rev.* **109**, 1492 (1958).
 - [7] B. I. Shraiman and E. D. Siggia, Mobile Vacancies in a Quantum Heisenberg Antiferromagnet. *Phys. Rev. Lett.* **61**, 467 (1988).
 - [8] S. Schmitt-Rink, C. M. Varma and A. E. Ruckenstein, Spectral function of holes in a quantum Antiferromagnet. *Phys. Rev. Lett.* **60**, 2793 (1988).
 - [9] C. L. Kane, P. A. Lee, and N. Read, Motion of a single hole in a quantum antiferromagnet. *Phys. Rev. B* **39**, 6880 (1989).
 - [10] P. W. Anderson, “Luttinger-liquid” behavior of the normal metallic state of the 2D Hubbard model. *Phys. Rev. Lett.* **64**, 1839 (1990).
 - [11] G. Martinez and P. Horsch, Spin polarons in the t - J model. *Phys. Rev. B* **44**, 317 (1991).
 - [12] Z. Liu and E. Manousakis, Spectral function of a hole in the t - J model. *Phys. Rev. B* **44**, 2414 (1991).
 - [13] E. Dagotto, Correlated electrons in high-temperature superconductors. *Rev. Mod. Phys.* **66**, 763 (1994).
 - [14] P. W. Leung and R. J. Gooding, Dynamical properties of the single-hole t - J model on a 32-site square lattice. *Phys. Rev. B* **52**, R15711 (1995).
 - [15] R. B. Laughlin, Evidence for quasiparticle decay in photoemission from underdoped cuprates. *Phys. Rev. Lett.* **79**, 1726 (1997).
 - [16] T. K. Lee and C. T. Shih, Dispersion of a single hole in the t - J model. *Phys. Rev. B* **55**, 5983 (1997).
 - [17] S. R. White and D. J. Scalapino, Hole and pair structures in the t - J model. *Phys. Rev. B* **55**, 6504 (1997).
 - [18] Z. Y. Weng, V. N. Muthukumar, D. N. Sheng, and C. S. Ting, Spin-charge separation in the single-hole-doped Mott antiferromagnet. *Phys. Rev. B* **63**, 075102 (2001).
 - [19] A.S. Mishchenko and N. Nagaosa, Electron-Phonon Coupling and a Polaron in the t - J Model: From the Weak to the Strong Coupling Regime, *Phys. Rev. Lett.* **93**, 036402 (2004).
 - [20] L. N. Bulaevskii, E. L. Nagaev, and D. L. Khomskii, A new type of auto-localized state of a conduction electron, *Sov. Phys. JETP* **27**, 836 (1968).
 - [21] B. O. Wells, Z. X. Shen, A. Matsuura, D. M. King, M. A. Kastner, M. Greven, and R. J. Birgeneau, E versus k Relations and Many Body Effects in the Model Insulating Copper Oxide $\text{Sr}_2\text{CuO}_2\text{Cl}_2$. *Phys. Rev. Lett.* **74**, 964 (1995).
 - [22] F. Ronning, C. Kim, D. L. Feng, D. S. Marshall, A. G. Loeser, L. L. Miller, J. N. Eckstein, I. Bozovic, and Z. X. Shen, Photoemission evidence for a remnant Fermi surface and a d-wave-like dispersion in insulating $\text{Ca}_2\text{CuO}_2\text{Cl}_2$. *Science* **282**, 2067 (1998).
 - [23] K.M. Shen, F. Ronning, D. H. Lu, W. S. Lee, N. J. C. Ingle, W. Meevasana, F. Baumberger, A. Damascelli, N. P. Armitage, L. L. Miller, Y. Kohsaka, M. Azuma, M. Takano, H. Takagi, and Z.-X. Shen, Missing quasiparticles and the chemical potential puzzle in the doping evolution of the cuprate superconductors, *Phys. Rev. Lett.* **93**, 267002 (2004).
 - [24] S. R. White, Density matrix formulation for quantum renormalization groups. *Phys. Rev. Lett.* **69**, 2863 (1992).
 - [25] K. Wu, Z. Y. Weng, and J. Zaanen, Sign structure of the t - J model. *Phys. Rev. B* **77**, 155102 (2008).
 - [26] S. R. White and D. J. Scalapino, Ground states of the doped four-leg t - J ladder, *Phys. Rev. B* **55**, R14701 (1997).
 - [27] S. R. White, private communication.
 - [28] H. C. Jiang, Z. Wang, and L. Balents, Identifying topological order by entanglement entropy, *Nature Physics* **8**, 902-905 (2012).
 - [29] C. Ye, P. Cai, R. Z. Yu, X. D. Zhou, W. Ruan, Q. Q. Liu, C. Q. Jin, and Y. Y. Wang, Visualizing the atomic scale electronic structure of the $\text{Ca}_2\text{CuO}_2\text{Cl}_2$ Mott insulator. arXiv:1201.0342.

Acknowledgements: Stimulating discussions with L. Balents, D. N. Sheng, S. R. White, J. Zaanen, and especially P. A. Lee are acknowledged. This work was partially supported by the KITP (NSF no. PHY05-51164) and the Center for Scientific Computing at the CNSI and MRL: the NSF MRSEC (DMR 1121053) and NSF CNS-0960316; by the NBRPC (nos. 2009CB929402, 2010CB923003, and 2011CBA00108); by the NSFC (no. 11174174) and the Tsinghua University ISRP (no. 2011Z02151).

Supplementary Information

In this supplemental material, we present some technical details.

Spin-spin correlations at half-filling. — At half-filling, the t - J model reduces to the Heisenberg model. For the isotropic Heisenberg coupled-chain systems, the behavior of the even-leg ladders is dramatically different from that of the odd ones. A well-known fact is that the even-leg ladders have a spin gap while the odd-leg ladders are gapless. The former leads to an exponential decay of the spin-spin correlation while the latter to a power law decay (see Fig. S1). The spin gap for the even-leg ladders is expected to vanish in the large leg number (namely two-dimensional) limit. Indeed, the spin structure factor in the 4-leg case has already exhibited strong antiferromagnetic correlations as shown in Fig. S2. These results are consistent with earlier DMRG work[30].

Some details of the hole density distribution. — Fig. S3 presents the contour plot of $\langle n_i^h \rangle$ for different ladders, $N = 40 \times N_y$ with $N_y = 2, 3, 4$, and 5. For each contour plot, we have checked numerically that the sum rule is satisfied, i.e., $\sum_i \langle n_i^h \rangle = 1$, where the summation is over all the sites.

A prominent feature can be clearly seen in these contour plots (see also Fig. S4 (B)). That is, for even-leg ladders there is a spatial oscillation on top of the localized density profile, while it is absent for odd-leg ladders. We wish to point out that this is concomitant with the parity effect of the spin-spin correlation shown in Fig. S1. In fact, the spin-gap effect is reduced as the hopping integral t increases, and eventually the parity effect disappears in the large t/J limit. Accordingly, the spatial oscillation of $\langle n_i^h \rangle$ must be diminished also in this limit. This prediction has been fully confirmed by numerical simulations, see Fig. S4 (B). In addition, we have observed that the localization length monotonically decreases as the ratio t/J increases, see the insets of Fig. S4. This suggests that the spin dynamics, governed by the superexchange J , does not play important roles in establishing the observed self-localization.

Electron and hole momentum distributions. — Fig. S5 shows the contour plot of the hole momentum distribution function $1 - n(\mathbf{k})$ for the 3-leg (A) and 4-leg (B) ladders, respectively at $N_x = 80$. The maximum of $1 - n(\mathbf{k})$ appears at $k_y = \pm\pi/2$ for the 4-leg ladder and $k_y = \pm 2\pi/3$ for the 3-leg ladder. The t/J -dependence of the hole momentum distribution is shown in Fig. S6. They show that the momentum distribution jump is monotonically reduced with the increase of t/J .

[30] S.R.White, R. M. Noack, and D. J. Scalapino, Resonating Valence Bond Theory of Coupled Heisenberg Chains. Phys. Rev. Lett. **73**, 886(1994).

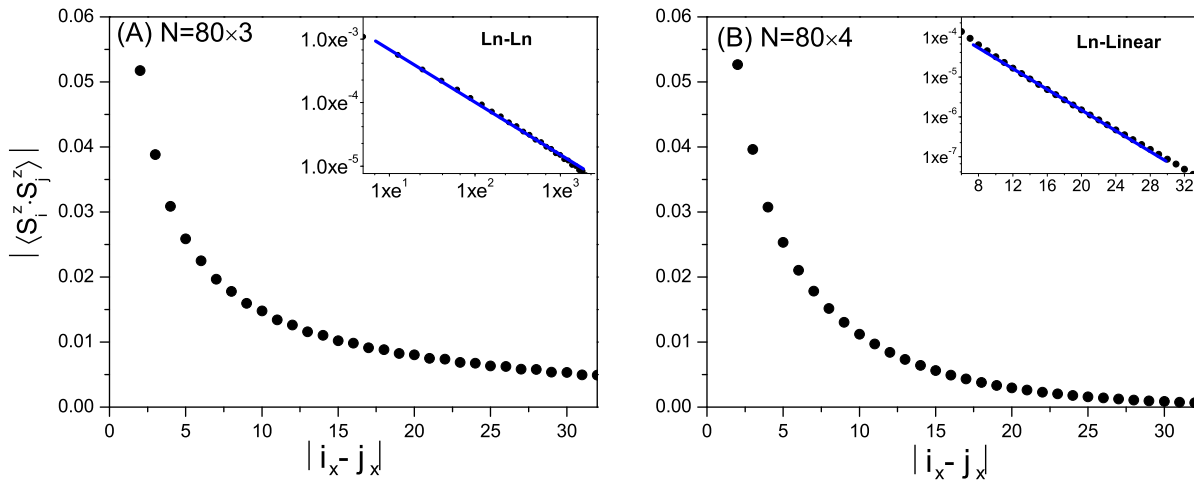


Fig. S1: The main panels are the spin-spin correlation $|\langle S_i^z S_j^z \rangle|$ in the 3-leg (A) and 4-leg (B) ladder, respectively. i_x and j_x are chosen to be on the middle leg of the corresponding ladder. The insets are ln-ln plot (A) and semi-ln plot (B). They are well fitted by straight (blue) lines, indicating a power law decay for the 3-leg ladder and an exponential decay for the 4-leg ladder.

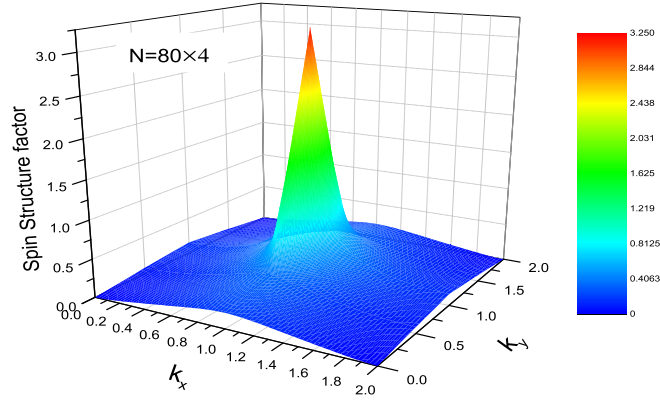


Fig. S2: Spin structure factor for the 4-leg ladder ($N=80 \times 4$). The peak is located at (π, π) , indicating strong spin antiferromagnetic correlations even though a finite spin gap is present.

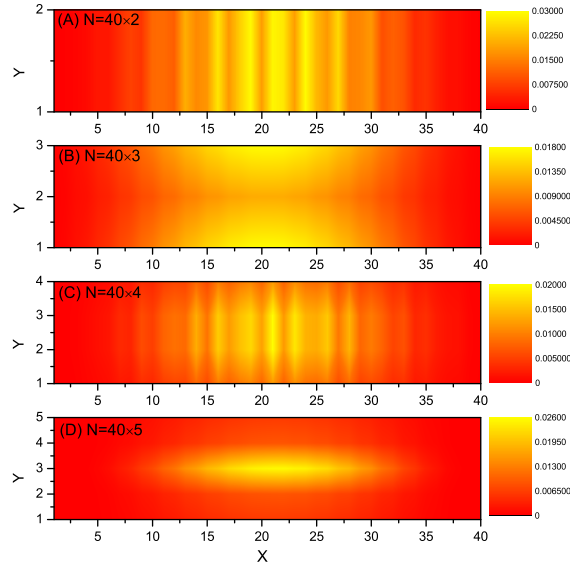


Fig. S3: Contour plots of the hole distribution in real space. The sample size 40×2 (A), 40×3 (B), 40×4 (C), and 40×5 (D) from top down.

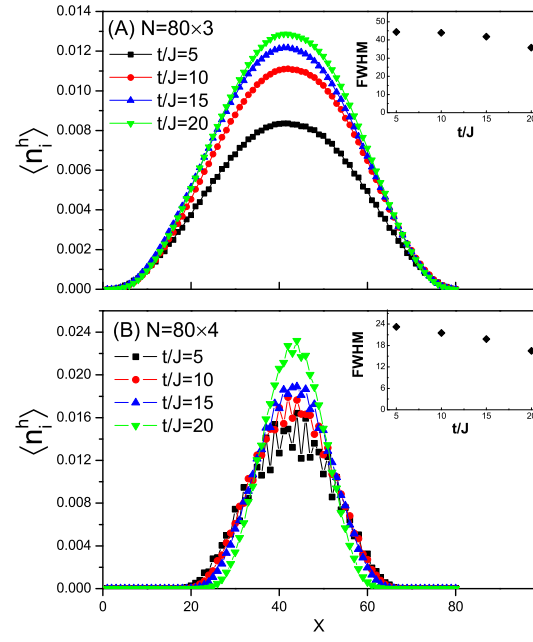


Fig. S4: The hole density profile $\langle n_i^h \rangle$ (with i located on the middle chain) at different ratios of t/J . The ladder size is 80×3 (A) and 80×4 (B). The localization length (the FWHM) is found to decrease as t/J increases (insets). Moreover, the amplitude of the spatial oscillation in the 4-leg ladder is suppressed as t/J increases, indicating that the behavior of even- and odd-leg ladders converges in the large t/J limit.

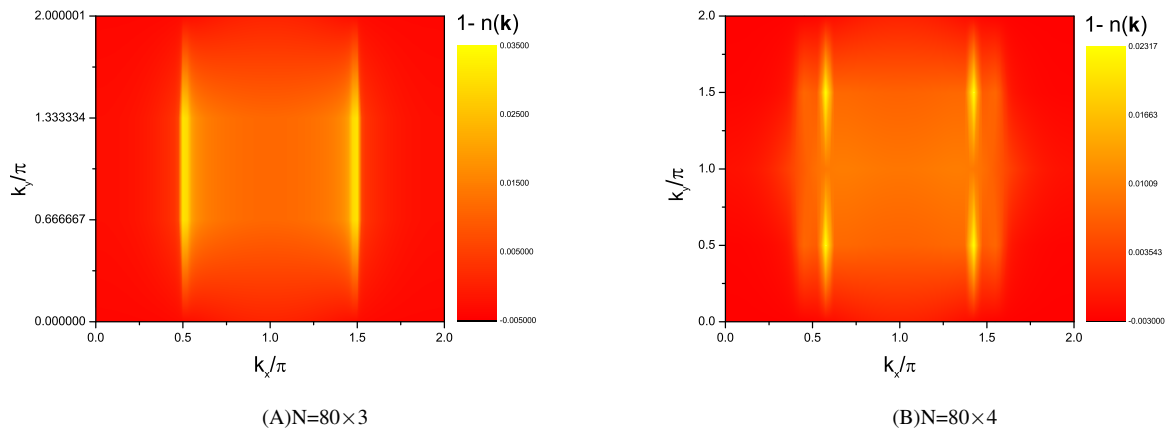


Fig. S5: Contour plots of the hole momentum distribution $1 - n(\mathbf{k})$ for 3-leg (A) and 4-leg (B) ladders.

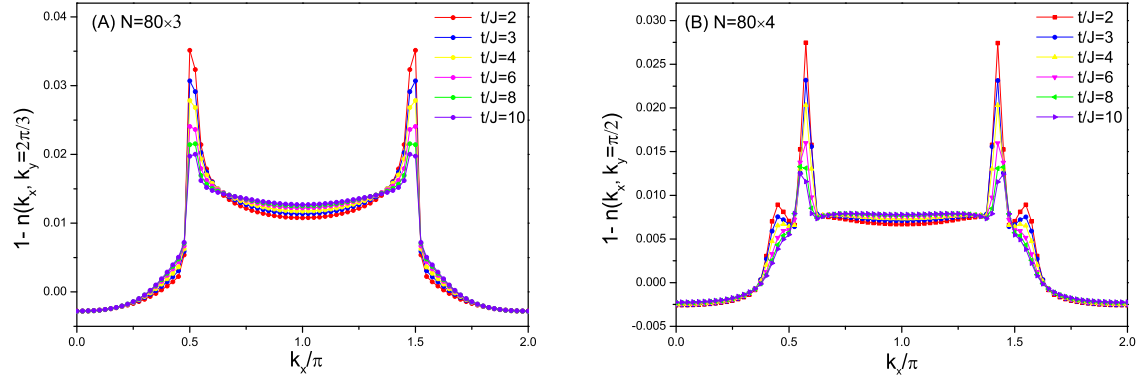


Fig. S6: The hole momentum distribution at different ratios of t/J for 3-leg (A) and 4-leg (B) ladders.